Atmos. Chem. Phys., 15, 9237–9251, 2015
www.atmos-chem-phys.net/15/9237/2015/
doi:10.5194/acp-15-9237-2015

Atmospheric Chemistry and Physics
Open Access

A comparison of measured HONO uptake and release with calculated source strengths in a heterogeneous forest environment

M. Sörgel[1,a], I. Trebs[2], D. Wu[3], and A. Held[1,4]

[1]Atmospheric Chemistry, University of Bayreuth, Bayreuth, Germany
[2]Environmental Research and Innovation (ERIN) Department, Luxembourg Institute of Science and Technology, Belvaux, Luxembourg
[3]Biogeochemistry Department, Max Planck Institute for Chemistry, Mainz, Germany
[4]Bayreuth Center of Ecology and Environmental Research, Bayreuth, Germany
[a]now at: Biogeochemistry Department, Max Planck Institute for Chemistry, Mainz, Germany

Correspondence to: M. Sörgel (m.soergel@mpic.de)

Received: 3 November 2014 – Published in Atmos. Chem. Phys. Discuss.: 23 January 2015
Revised: 9 July 2015 – Accepted: 24 July 2015 – Published: 20 August 2015

Abstract. Vertical mixing ratio profiles of nitrous acid (HONO) were measured in a clearing and on the forest floor in a rural forest environment. For the forest floor, HONO was found to predominantly deposit, whereas for the clearing, net deposition dominated only during nighttime and net emissions were observed during daytime. For selected days, net fluxes of HONO were calculated from the measured profiles using the aerodynamic gradient method. The emission fluxes were in the range of 0.02 to 0.07 nmol m^{-2} s^{-1} and thus were in the lower range of previous observations. These fluxes were compared to the strengths of postulated HONO sources. Laboratory measurements of different soil samples from both sites revealed an upper limit for soil biogenic HONO emission fluxes of 0.025 nmol m^{-2} s^{-1}. HONO formation by light-induced NO_2 conversion was calculated to be below 0.03 nmol m^{-2} s^{-1} for the investigated days, which is comparable to the potential soil fluxes. Due to light saturation at low irradiance, this reaction pathway was largely found to be independent of light intensity, i.e. it was only dependent on ambient NO_2.

We used three different approaches based on measured leaf nitrate loadings for calculating HONO formation from HNO_3 photolysis. While the first two approaches based on empirical HONO formation rates yielded values in the same order of magnitude as the estimated fluxes, the third approach based on available kinetic data of the postulated pathway failed to produce noticeable amounts of HONO. Estimates based on reported cross sections of adsorbed HNO_3 indicate that the lifetime of adsorbed HNO_3 was only about 15 min, which would imply a substantial renoxification. Although the photolysis of HNO_3 was significantly enhanced at the surface, the subsequent light-induced conversion of the photolysis product NO_2 did not produce considerable amounts of HONO. Consequently, this reaction might occur via an alternative mechanism.

By explicitly calculating HONO formation based on available kinetic data and simple parameterizations, we showed that (a) for low NO_x the light-induced conversion of NO_2 on humic acids is already light saturated by the early morning, (b) HONO formation from photolysis of adsorbed HNO_3 appears to proceed via an alternative mechanism and (c) estimates of HONO emissions from soil are very sensitive to mass transfer and acidic soils do not necessarily favour HONO emissions.

1 Introduction

Gaseous nitrous acid (HONO) may contribute up to ∼ 80 % to the primary formation of hydroxyl radicals (OH), which play a key role in the degradation of most air pollutants (Kleffmann et al., 2005, Kleffmann, 2007; Volkamer et al., 2010). The source of OH radicals is the photolysis of HONO (Reaction R1):

$$\mathrm{HONO} + h\nu (< 400\,\mathrm{nm}) \rightarrow \mathrm{NO} + \mathrm{OH} \quad \text{(R1)}$$

$$NO + OH + M \rightarrow HONO + M \quad \text{(R2)}$$

$$HONO + OH \rightarrow NO_2 + H_2O \quad \text{(R3)}$$

The back Reaction (R2) consumes OH and regenerates HONO. Reaction (R3) is typically a minor loss term for HONO (e.g. Su et al., 2008; Sörgel et al., 2011a; Oswald et al., 2015) and OH due to the low concentrations of both reaction partners. Solely considering Reactions (R1) to (R3), HONO is an OH radical reservoir as discussed for urban plumes (Lee et al., 2013). If Reactions (R1) to (R3) are in equilibrium, a photo stationary state (PSS) is established (e.g. Cox, 1974; Kleffmann et al., 2005). In the case an additional efficient HONO loss term exists (e.g. deposition) (Harrison et al., 1996; Wong et al., 2011; VandenBoer et al., 2013), HONO formation is a sink for OH radicals. For instance it was shown that plants (Schimang et al., 2006) and soils (Donaldson et al., 2014a) efficiently take up HONO. However, if additional sources of HONO exist that exceed the loss terms, HONO is a source for OH radicals.

A well-known source of HONO is the heterogeneous disproportionation of NO_2, forming HONO and HNO_3:

$$2NO_2 + H_2O \rightarrow HONO + HNO_3 \quad \text{(R4)}$$

Although Reaction (R4) is well-known, its mechanism is still unclear. A potential mechanism involving the dimer of NO_2 was proposed by Finlayson-Pitts and colleagues (Finlayson-Pitts et al., 2003), and has been further analysed using theoretical approaches (Miller et al., 2009; De Jesus Medeiros and Pimentel, 2011). This reaction was found to be too slow to explain daytime HONO mixing ratios well above the PSS (e.g. Kleffmann et al., 2005; Sörgel et al., 2011a; Wong et al., 2013). However, it is linked to the nighttime accumulation of HONO, which triggers early morning photochemistry (Alicke et al., 2003). Other light-independent mechanisms for NO_2 conversion to HONO, such as the reduction by organics (Gutzwiller et al., 2002) and chemisorption on mineral surfaces (Gustafsson et al., 2008), were also proposed. These reactions have not yet been quantified under field conditions and concerns exist whether or not chemisorption would take place under ambient conditions (Finnlayson-Pitts, 2009). Furthermore, NO_2 reduction on soot was found to be quickly deactivated (Kleffmann et al., 1999; Arens et al., 2001; Aubin and Abbatt, 2007).

As the observed HONO mixing ratios almost always exceed those calculated from the PSS assumption (summarized by Kleffmann, 2007, and Volkamer et al., 2010), numerous attempts to identify HONO sources driven by light or by temperature that can overcome the loss by photolysis were made. Recently, it was found that the heterogeneous disproportionation (R4) can be catalysed by anions that are formed during photooxidation in the atmosphere (Yabushita et al., 2009; Colussi et al., 2013). Light enhancement of Reaction (R4) has also been attributed to HNO_3 photolysis (Ramazan et al., 2004), and photolysis of adsorbed HNO_3 on natural surfaces was proposed as an important HONO source in the atmosphere (Zhou et al., 2002, 2003, 2011).

In contrast to HONO formation observed on natural surfaces (Zhou et al., 2003, 2011), HONO has not been detected as a primary reaction product of HNO_3 photolysis in laboratory studies up to now (Zhu et al., 2010, Schuttlefield et al., 2008, Rubasinghege and Grassian, 2009; Abida et al., 2012). Most studies (Zhu et al., 2010, Schuttlefield et al., 2008, Abida et al., 2012) report NO and NO_2 as the main products of this reaction (Rubasinghege and Grassian, 2009). The formation of NO_2 and NO_2* is also proposed as an alternative mechanism, which involves photolysis of complexes of either HNO_3 or NO_3^- and NO_2 or N_2O_4, respectively (Kamboures et al., 2008). Recent studies applying a novel laser-based technique (Zhu et al., 2010, Abida et al., 2012) identified excited NO_2* as the main photolysis product of adsorbed HNO_3 and, furthermore, confirmed an enhanced absorption cross section of adsorbed HNO_3 compared to gas-phase HNO_3. Potentially, NO_2* reacting with water vapour can produce HONO, but this reaction does not result in significant amounts of HONO under atmospheric conditions (Crowley and Carl, 1997; Sörgel et al., 2011a; Amedro et al., 2011). Hence, Zhou et al. (2011) suggested that NO_2 formed during HNO_3 photolysis further reacts via the mechanism proposed by Stemmler and colleagues (Stemmler et al., 2006, 2007), where solid organic material such as humic acid (HA) acts as a photosensitizer and reduces NO_2 (George et al., 2005). Photosensitized reactions may be a promising pathway for explaining daytime HONO formation as hypothesized from correlations of the unknown HONO source with the photolysis frequency of NO_2, $j(NO_2)$, or irradiance (e.g. Su et al., 2008; Sörgel et al., 2011a; Wong et al., 2012). The photolysis of o-nitrophenols was also proposed as a HONO source (Bejan et al., 2006) that however has not yet been quantified in field measurements. As it depends on the amount of nitrophenols in air, this source is expected to be more important for polluted urban conditions (Bejan et al., 2006).

A process directly driven by temperature could be the volatilization of HONO from soil nitrite (Kubota and Asami, 1985; Su et al., 2011). The temperature dependence of this process has been attributed to the temperature dependence of the Henry's law equilibrium between soil–solution and soil–air interfaces (Su et al., 2011). Additionally, it was suggested that HONO emissions are driven by ammonia-oxidizing bacteria in soil, whose activity also depends on temperature (Oswald et al., 2013). Nitrogen availability for microorganisms was found as a limiting factor for HONO emissions from natural soils (Maljanen et al., 2013). HONO deposition during night and re-emission that is driven by acid displacement (VandenBoer et al., 2015) during daytime has been proposed to explain the missing daytime source (VandenBoer et

al., 2013). The physicochemical interactions with soil particles have been analysed in more detail by Donaldson et al. (2014a, b).

Regardless of the mechanism, the ground surface has been proposed as a major source of HONO (e.g. Febo et al., 1996; Stutz et al., 2002; Zhang et al., 2009; Sörgel et al., 2011b; Wong et al., 2012, 2013; VandenBoer et al., 2013), although there is a potential contribution from other heterogeneous sources within the boundary layer (Zhang et al., 2009; Wong et al., 2013). Flux measurements of HONO (Zhou et al., 2011; Ren et al., 2011) reported strong daytime upward fluxes, thus confirming a ground source. In contrast, a recent study (Li et al., 2014) based on concentration measurements of HONO in the residual layer and the mixed layer proposed that an internal recycling mechanism (reaction between NO_x and HO_x) is mainly responsible for HONO formation.

In this study, we present vertical mixing ratio profiles of HONO measured close to the ground surface (< 2 m) in a clearing and on the forest floor in a heterogeneous forest landscape in order to identify sources and sinks of HONO in natural environments. Under favourable conditions, our setup can be used to derive estimates of the surface fluxes of HONO by the aerodynamic gradient method. These fluxes are compared to best estimates of HONO source strengths of three proposed mechanisms derived from measured quantities: (a) soil HONO emissions, (b) photosensitized NO_2 conversion, and (c) HNO_3 photolysis.

2 Experimental

Vertical mixing ratio profiles of HONO, nitrogen oxides (NO_x), and ozone were measured in a clearing and on the forest floor at the Waldstein ecosystem research site in the Fichtel Mountains, NE Bavaria (Germany) in 2011 and 2012 as part of the Exchange processes in mountainous regions (EGER) research project (Foken et al., 2012). The profile measurements were made in June–July 2011 (intensive observation period IOP-3) in the Köhlerloh clearing (50°08′22.3″ N, 11°52′01.5″ E), and in August–September 2012 (IOP-4) on the forest floor about 290 m north of the clearing site close to the main tower (50°08′31.2″ N, 11°52′00.8″ E; 775 m a.s.l.) of the Weidenbrunnen site. Meteorological variables for the comparison of both campaigns were taken from the Pflanzgarten site, which is 280 m north-west of the main tower and 490 m north–north-west of the clearing site. An aerial view of the different sites can be found in the Supplement (Fig. S1).

HONO was measured using a commercially available long path absorption photometer (LOPAP, QUMA, Wuppertal, Germany) with a time resolution of 3 min. A detailed description of the instrument is provided by Heland et al. (2001) and Kleffmann et al. (2002). The instrument was placed on a scaffold in a ventilated aluminium box as described by Sörgel et al. (2011b). The limit of detection (3σ of zero air noise) ranged from 1 to 7 ppt. NO and NO_2 were measured by chemiluminescence (Model 42i-TL Thermo Scientific, Franklin, MA, USA) using a specific photolytic converter for NO_2 (Droplet Measurement Technologies, Boulder, CO, USA). The limit of detection was 50 ppt for NO and about 140 ppt for NO_2. Trace gas profiles of HONO, NO, and NO_2 were obtained by moving the external sampling unit of the LOPAP and an inlet line for NO_x to five (0.1, 0.2, 0.4, 0.8 and 1.6 m) or three (0.1, 0.4 and 1.6 m) different heights using an automated lift system (Fig. S2). The dwell time at each height was 6 and 7 min in IOP-3 and 9 min (IOP-4), which allowed sufficient sampling periods with respect to the time resolution of the LOPAP (1–2 data points). All data of the lift system (NO_x, HONO, temperature and lift position) were recorded every 20 s. Additionally, eddy covariance measurements were made during IOP-3 with a CSAT3 sonic anemometer (Campbell Scientific, Logan, UT, USA) located at a height of 2.25 m on a mast about 20 m north-west of the profile measurements. During IOP-4, a sonic anemometer (Model 81000, R. M. Young, Traverse City, MI, USA) was located about 2 m east of the profile measurements at a height of 2 m. The friction velocity (u_*) was calculated with TK3 software (Mauder and Foken, 2011). Air temperature was measured by radiation shielded and ventilated Pt-100 sensors with a resolution of 0.1 K at 1.4 m (1.6 m in IOP-4) and 0.1 m above ground level. Soil temperature was monitored with a Pt-100 sensor at a depth of 2 cm.

At the Pflanzgarten site, air temperature and relative humidity (RH) were measured with HMP45 sensors (Vaisala, Helsinki, Finland) at a height of 2 m, precipitation was measured with an OMC-212 rain gauge (Observator Instruments, Ridderkerk, the Netherlands), and solar global irradiance was measured on the roof of the measurement container with a CM5 pyranometer (Kipp and Zonen, Delft, the Netherlands). HONO photolysis frequency, j(HONO), was calculated from global radiation according to Trebs et al. (2009).

Spectral irradiance and photolysis frequencies were calculated using the Tropospheric Ultraviolet and Visible (TUV) radiation model (Madronich and Flocke, 1998) version 5.0. Additional information about methods and instruments can be found in the Supplement.

3 Results and discussion

3.1 Meteorological conditions and comparison of sites

As shown in Fig. 1, the range of air temperature at the Pflanzgarten site was comparable for both campaigns and ranged between about 5 and 27 °C. The maximum temperatures were 27.3 °C for IOP-3 and 25.8 °C for IOP-4, respectively. The minimum temperature of the June–July period (IOP-3) was lower (5.5 °C) than during IOP-4 in September (6.0 °C). Mean values (and standard deviations) were 14.7 ± 5.1 °C for IOP-3 and 14.2 ± 4.4 °C for IOP-4. Ac-

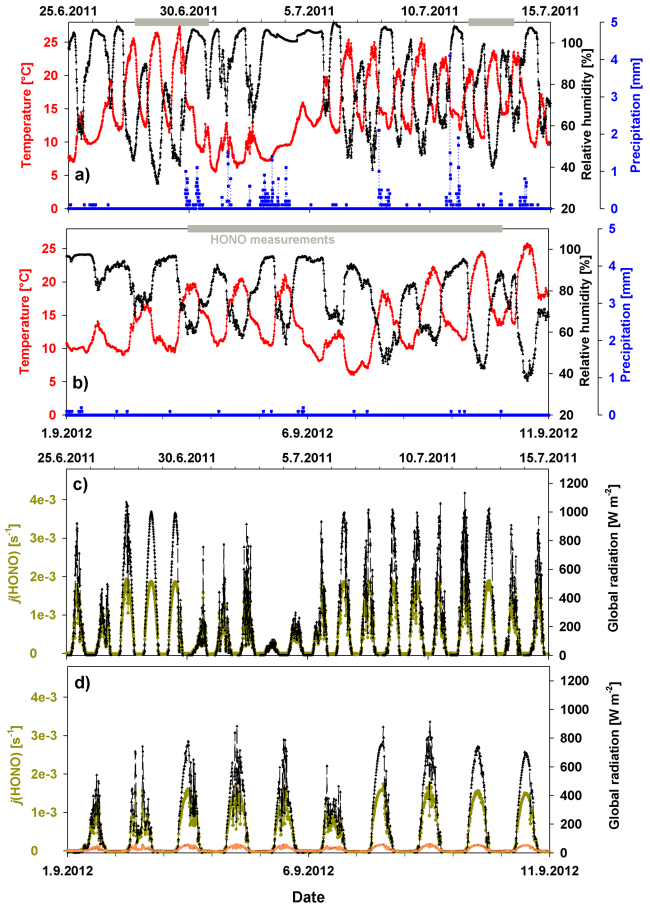

Figure 1. Temperature (red), relative humidity (RH, black) and precipitation (blue) averaged for a 10 min interval are shown in panels **(a)** for 25 June to 15 July 2011 (IOP-3), and **(b)** for 1 September 2012 to 11 September 2012 (IOP-4). Periods when HONO vertical profiles were measured are indicated by grey bars at the top of the graphs. Panels **(c)** and **(d)** show solar global irradiance (black) and j(HONO) in dark yellow, calculated according to Trebs et al. (2009), for the respective campaigns. Additionally, j(HONO) at the forest floor (orange) was calculated by applying a factor of 10 taking into account attenuation by the canopy (Sörgel et al., 2011b). All data were taken from the Pflanzgarten site.

cordingly, RH values cover similar ranges from about 30 to 100 % with somewhat higher values in the summer campaign due to frequent rain events (i.e. an average precipitation of 1.8 mm d^{-1} in IOP-3 and 0.3 mm d^{-1} in IOP-4). The long-term monthly means (1971–2000) at this site are 3.6 mm d^{-1} for June, 4.1 mm d^{-1} in July and 2.8 mm d^{-1} in September (Foken, 2003). Consequently, both periods exhibited less precipitation than the long-term average, although frequent but light rain events occurred during IOP-3, whereas in September (IOP-4) precipitation events were rare. Maximal RH values are slightly different for the two IOPs and range from 95 to ∼ 100 %. The values greater than 100 % have to be viewed with caution as the sensor accuracy in the range from 90 % RH to 100 % RH is ±3 % and the sensor is not able to measure accurately if water is condensing at high humidity. Global radiation, and thus j(HONO), was higher in June–July 2011 than in September 2012. Correspondingly, the calculated j(HONO) values show maxima of 2×10^{-3} s^{-1} in 2011 and 1.8×10^{-3} s^{-1} in 2012. The radiation and photolysis frequencies at the forest floor are a factor of 10 to 40 lower than above the canopy depending on the time of day and canopy structure (Sörgel et al., 2011b). J(HONO) values calculated by applying a factor of 10 are shown in Fig. 1d. Since weather conditions were comparable, major differences between the two campaigns are expected to be due to (a) availability of radiation, (b) turbulent exchange and (c) ground cover. Radiation and turbulent exchange are reduced at the forest site below the canopy compared to the open clearing. The ground cover at the clearing was dominated by grass and blueberry plants, while the forest floor was mainly covered by moss.

3.2 HONO mixing ratio differences and estimated net fluxes

NO mixing ratios at the 1.6 m level were generally low, especially during nighttime. Average mixing ratios were 0.2 ppb during the first period in 2011 (Fig. 2a), 0.1 ppb during the second period in 2011 (Fig. 2b), and 0.05 ppb in 2012 (Fig. 3a). Due to the well-known soil NO emissions (e.g. Ludwig et al., 2001; Bargsten et al., 2010) caused by microbiological activity, NO mixing ratios were higher at 0.1 m. The average mixing ratios close to the ground (Figs. S3 to S5) at 0.1 m were 0.75 ppb during the first period, 0.5 ppb during the second period in 2011, and 0.1 ppb in 2012. Average NO_2 mixing ratios at the upper level were 1.7 ppb (min. 0.3 ppb and max. 3 ppb) during the first period, 1.1 ppb (min. 0.2 ppb and max. 2.4 ppb) during the second period in 2011, and 1.6 ppb (min. 0.2 ppb and max. 4.8 ppb) in 2012. Average HONO mixing ratios at the 1.6 m level were 94 ppt (min. 12 ppt and max. 308 ppt) during the first period, 80 ppt (min. 30 ppt and max. 316 ppt) during the second period in 2011, and 90 ppt (min. 26 ppt and max. 257 ppt) in 2012.

Since vertical mixing ratio differences are the result of the competition between sources and sinks as well as of transport dynamics, Figs. 2 and 3 additionally show vertical temperature differences and the friction velocity u_*. Temperature differences reflect atmospheric stability and u_* is a measure of the intensity of turbulent exchange. A typical diurnal cycle caused by radiative heating and cooling of the surface was observed at the clearing, with stable conditions (positive temperature differences) during the night and unstable conditions during the day. The temperature differences between 0.1 and 1.4 m above the ground were up to 6 K during the night and up to −4 K during the day. During stable conditions, u_* dropped and mixing ratio differences increased due to suppressed transport. In the clearing, very stable and calm conditions caused large HONO and NO (not shown) mixing

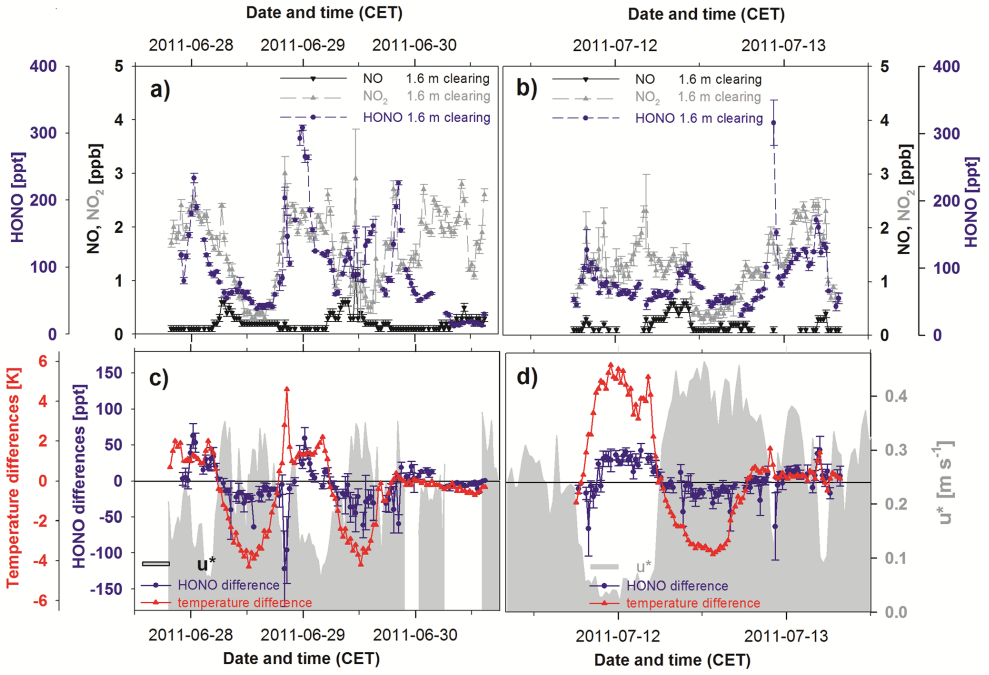

Figure 2. HONO (blue), NO (black) and NO_2 (grey) mixing ratios measured at the clearing at 1.6 m averaged for each height interval (i.e. omitting the first data points according to the time resolution of the instruments) from panels **(a)** 27 June to 30 June 2011 (NO_x: 3.5 min mean; HONO: 3 min mean), and **(b)** 11 July to 13 July 2011(NO_x: 4 min mean; HONO: 3 min mean). Missing NO values are below the limit of detection ($LOD_{2\sigma} = 50$ ppt). Vertical temperature differences (red triangles and line) and HONO mixing ratio differences (blue dots and line) for each cycle ($\sim$ 30 min) are shown in panels **(c)** and **(d)** as well as the friction velocity (30 min mean) in grey shading. Differences of mean HONO values measured at 1.6 and 0.1 m are presented and error bars denote combined standard deviations. For temperature, differences between 1.4 and 0.1 m are shown.

ratio differences during sunset. Below the canopy at the forest site, diurnal cycles of stability are typically opposite to those observed at the clearing (Foken, 2008). However, the observed temperature differences do not feature a clear diurnal pattern and differences are generally an order of magnitude lower than at the clearing. This can be explained by the reduced heating of the forest floor and the reduced radiative cooling due to the shading of the canopy. As wind speed is reduced by the canopy as well, the friction velocity is on average a factor of 3–4 lower. Maximal values of u_* were 0.46 m s^{-1} in the clearing and 0.16 m s^{-1} on the forest floor, respectively. HONO differences in the clearing (1.6 to 0.1 m) shown in Fig. 2c and d feature distinct diurnal cycles with positive gradients at night indicating net deposition and negative gradients during day indicating net emission. On the forest floor, HONO differences were either positive or close to zero, i.e. net emission was not observed (Fig. 3b).

We calculated net HONO fluxes from selected profiles using the aerodynamic gradient technique (Wolff et al., 2010). Despite the fact that u_* was measured at 2.25 m on a separate tower about 20 m from the profile measurements at the clearing, the measurements were influenced by the same ground cover (dimensions of clearing $\sim 300 \times 400$ m). At the forest floor both measurements were collocated ($\sim$ 2 m distance and u_* measured in 2 m height). Mixing ratio differences were considered to be representative for the air layer between 1.6 and 0.1 m at the forest floor, but at the clearing, differences between 1.6 m and 0.4 were were used (for flux calculations), as 0.1 m was below the zero-plane displacement height (d).

The calculated daytime net emission fluxes of HONO at the clearing were in the range of 0.01 to 0.07 nmol m^{-2} s^{-1} (mean 0.04 ± 0.02 nmol m^{-2} s^{-1}; $N = 17$). This is about a factor of 3 lower than fluxes reported for another rural forested site (Zhou et al., 2011; Zhang et al., 2012) and about an order of magnitude lower than for semi-rural and urban sites (Harrison and Kitto, 1994; Harrison et al., 1996; Ren et al., 2011). However, these fluxes are higher than the values observed at Blodgett Forest (Ren et al., 2011). The mean HONO net emission flux estimate of 0.04 nmol m^{-2} s^{-1} with a corresponding mixing ratio of 65 ppt at 1.6 m at the clearing compares reasonably well with the somewhat lower fluxes at Blodgett Forest (flux < 0.01 nmol m^{-2} s^{-1}; 20–30 ppt) and with the somewhat higher fluxes at the Program for Research on Oxidants: PHotochemistry, Emissions, and Transport (PROPHET) site (mean flux 0.19 nmol m^{-2} s^{-1}; 70 ppt). The low fluxes at Blodgett Forest have been attributed to the alkalinity of the soil, which, according to acid–base and

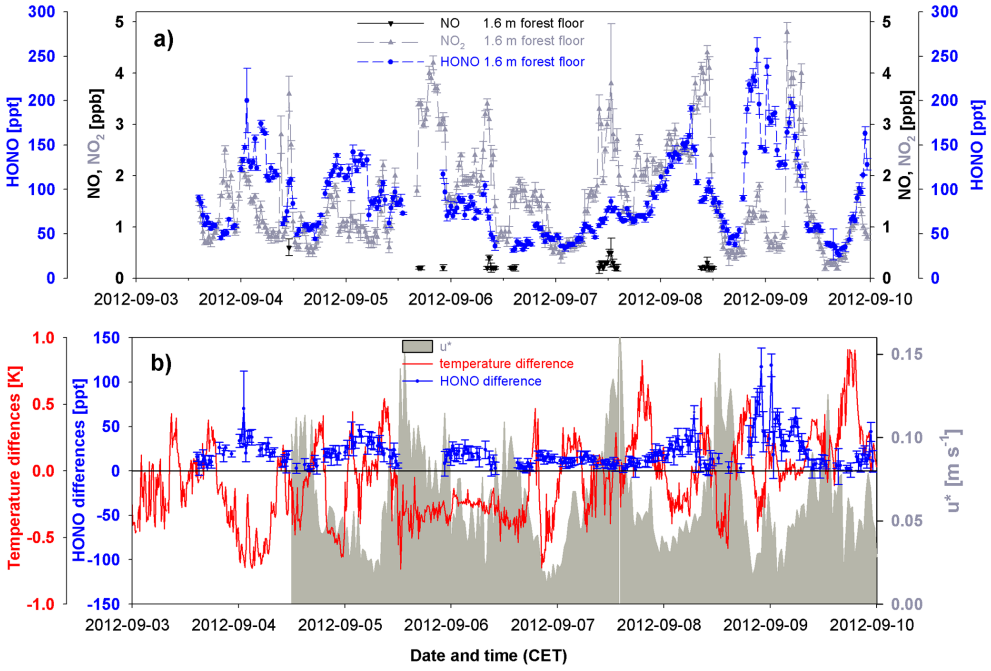

Figure 3. HONO (blue), NO (black) and NO_2 (grey) mixing ratios measured at the forest floor at 1.6 m averaged for each height interval (i.e. omitting the first data points according to the time resolution of the instruments) from 3 to 9 September 2012 (NO_x: 7 min mean; HONO: 6 min mean) are shown in panel **(a)**. Missing NO values are below the limit of detection ($LOD_{2\sigma} = 50$ ppt). Vertical temperature differences (red line) and HONO mixing ratio differences (blue dots and line) for each cycle ($\sim$ 30 min) are shown in panel **(b)** as well as the friction velocity (30 min mean) in grey shading. Differences of mean HONO values measured at 1.6 and 0.1 m are presented and error bars denote combined standard deviations. For temperature, differences between 1.6 and 0.1 m are shown.

Henry's law equilibrium (Su et al., 2011), should enhance HONO uptake or hinder its release. The calculated fluxes indicate the existence of a daytime ground source, whose strength is of a comparable order of magnitude to that found in other studies in rural forested areas. Nighttime net deposition fluxes (0.006 ± 0.003 nmol m^{-2} s^{-1}; $N = 12$) were about a factor of 7 lower than daytime net emission fluxes at the clearing (see Sect. 3.3.1).

At the forest floor, only net deposition was observed with fluxes varying between zero and about 0.012 nmol m^{-2} s^{-1} (mean: 0.004 ± 0.003; $N = 52$) for the selected days (4–7 September 2012). Hence, net deposition fluxes at the forest floor were comparable to nighttime net deposition at the clearing. Assuming that daytime deposition fluxes at the clearing are within the same range, emission fluxes at the clearing are at least about 15 % higher than the net fluxes. If considerable stomatal uptake of HONO occurs, as proposed by Schimang et al. (2006), the daytime deposition will be much higher than during nighttime due to stomatal aperture. Hence, to sustain the observed net emission fluxes, HONO emissions from the ground need to be even higher.

It should be noted that the derived fluxes should be considered as rough estimates for several reasons. The profiles were measured sequentially and not simultaneously at the different heights. Hence, only profiles under stationary conditions were evaluated, i.e. when mixing ratio changes between two profile cycles were small at each measurement height. This was mainly the case from 22:00 to 04:00 CET during night and from 11:00 to 15:00 during day. Furthermore, the mixing ratio differences during daytime were rather small (5 to 26 ppt; mean 14 ppt). The differences were 1.3 to 8.5 times the standard deviation of the mean values at one height and larger than the combined errors (sum of standard deviations of both heights). Differences that were smaller than the combined standard deviation were omitted for the flux calculations. Besides the uncertainty in the mixing ratio differences, the estimate of the zero-plane displacement height d has considerable influence on the fluxes. We used $d = 0.7$ times the canopy height (Foken, 2008) with a canopy height of 0.25 m of the surrounding blueberry canopy (E. Falge, 2014, personal communication) at the clearing. As roughness elements (like deadwood, blueberry plants, small spruce and grass) were distributed very inhomogeneously, it is unclear if the applied displacement height is appropriate and would hold for all wind directions. If the chosen canopy height was instead 0.4 m, the fluxes would decrease by about 20 %. Compared to the errors of the mixing ratio differences and of the displacement height, the error in u_* is expected to be negligible. At the forest floor we measured at a flat surface covered with moss that has a comparably low roughness

($d = 0.007$ m), thus the fluxes are less sensitive to small differences in d.

3.3 HONO sinks

3.3.1 Deposition

Except for the uptake of HONO by aerosol surfaces, no considerable gas-phase HONO sinks exist in the absence of light. This implies that dry and wet deposition are the most important loss pathways in the dark.

Net deposition means that although HONO formation by either heterogeneous disproportionation of NO_2 or direct soil emission may take place, net deposition is observed because the production of HONO is smaller than the loss by deposition. For our study, soil emissions can be neglected (see Sect. 3.4.1). Calculated nighttime deposition velocities of 0.08 to 0.5 cm s^{-1} (mean 0.24 ± 0.13) at the clearing were in the lower range of reported values at 0.08 to 6 cm s^{-1} (Harrison and Kitto, 1994; Harrison et al., 1996; Stutz et al., 2002).

At the forest floor, deposition was the dominating process both day and night. The vertical profiles (Fig. 3b) do not provide evidence that HONO emission from the ground surface takes place because the differences are either positive or ambiguous within the uncertainty range. The HONO deposition velocities ranged from 0.03 to 0.4 (mean 0.16 ± 0.08 cm s^{-1}), which is in the lower range of previously reported values (e.g. Harrison et al., 1996, Stutz et al., 2002) and a factor of 1.5 lower than at the clearing. To our knowledge, measured HONO fluxes at forest floors have not been reported up to now.

In a modelling study, Wong et al. (2011) pointed out that nighttime deposition is an important part of HONO cycling, which was recently confirmed by vertical profile measurements (VandenBoer et al., 2013). VandenBoer et al. (2013) proposed that the deposited HONO might form a reservoir that is re-emitted during the day and can thus explain a significant fraction of the missing daytime source. For the forest floor, we can exclude the possibility that this pathway is a general source of HONO because no emissions were observed. This is in line with laboratory studies, which showed that HONO can be taken up by plants (Schimang et al., 2006) and soil (Donaldson et al., 2014a). Due to the limited available data, we cannot exclude the possibility that re-emission may occasionally take place. However, we showed that net deposition (even if it is small) persists during the day at the forest floor during our measurement period. Thus, sources and sinks coexist over small spatial scales, which has to be taken into account for measurements at elevated levels that integrate over larger areas (horizontal heterogeneity), as well as for measurements above the canopy (vertical heterogeneity).

3.3.2 Photolysis

Photolysis has been identified as the dominating HONO loss process during the day (e.g. Kleffmann, 2007; Su et al., 2008; Sörgel et al., 2011a; Wong et al., 2013; VandenBoer et al., 2013; Oswald et al., 2015). We calculated the HONO loss rates from photolysis frequencies and HONO mixing ratios within a boundary layer height of 1000 m in two different ways: (a) the measured HONO mixing ratio at 1.6 m was used for the entire volume or (b) we assumed a linear HONO profile throughout the boundary layer to account for elevated HONO levels close to the ground as observed by Zhang et al. (2009) and VandenBoer et al. (2013). The artificial linear HONO profile was created using the measurements at 1.6 m and a background level (free troposphere) of 10 ppt (Zhang et al., 2009). The geometric mean of these values was used to calculate the HONO loss within the boundary layer volume. Using these two simplified approaches yields loss rates of (a) 0.2–1 ppb h^{-1} and (b) 0.08–0.5 ppb h^{-1}. These values are within the range of values reported for the unknown HONO source (e.g. Kleffmann, 2007). This is not surprising because the photolytic loss and the unknown source were found to be the dominant terms of the HONO budget for low NO_x levels (e.g. Sörgel et al., 2011a; Oswald et al., 2015), i.e. in the absence of other sources and sinks the photolytic loss equals the unknown source. Integrating the photolytic loss term over a boundary layer height of 1000 m and converting it into a surface flux yields mean fluxes of (a) 4.6 nmol m^{-2} s^{-1} and (b) 2 nmol m^{-2} s^{-1} respectively, which is a factor 100 and 40 higher than the mean emission flux derived from the measurements at the clearing (see Sect. 3.2). Consequently, the contribution of the surface emissions to the HONO source would be in the order of a few percent. This is in agreement with a proposed internal volume source (Li et al., 2014) and estimates of ground source contributions of about 20 % derived from measured boundary layer profiles (Zhang et al., 2009; Li et al., 2014). Close to the ground (lowest 35 m), a contribution of more than 60 % was found in modelling studies (Czader et al., 2012; Wong et al., 2013). As these studies were conducted in the urban area of Houston (Texas, USA), which is characterized by higher direct HONO emissions and higher levels of NO_x compared to our site, the relative contribution of the ground source in the lowest 35 m might be higher for our site. Nevertheless, the contribution was reduced to about 50 % by integrating the lowermost 300 m (Wong et al., 2013) and, therefore, integrating over a boundary layer height of 1000 m will further reduce this contribution. As none of the other boundary layer profile measurements have been analysed with a chemistry-transport model up to now, it remains unclear if the differences in HONO budgets (ground versus gas phase) are real or are caused by the different assumptions and simplifications in the different approaches.

3.4 HONO ground sources

The existence of a HONO ground source was confirmed by profile (e.g. Zhang et al., 2009; VandenBoer et al., 2013) and flux measurements (Zhou et al., 2011; Ren et al., 2011). In the following we compare the measured ground source to estimates for three different proposed formation mechanisms based on measured quantities.

3.4.1 Soil emissions

For both the forest and the clearing site, a set of soil samples was collected from two different ground cover types (blueberry and moss within the forest and blueberry and grass in the clearing) and potential HONO emission fluxes were measured using a dynamic chamber in the laboratory (for details see the Supplement). HONO fluxes were mostly within the calculated uncertainty range (Fig. S6). The sample taken directly below the lift system at the clearing (sample 4, Fig. S6) was the only sample for which potential emissions were observed. From those measurements we derive an upper limit for the HONO soil emission flux of $0.025 \pm 0.015\,\mathrm{nmol\,m^{-2}\,s^{-1}}$. This flux also represents an upper limit with regard to the experimental conditions as the chamber was flushed with zero air and the samples were measured at 25 °C. During the field measurements, the soil temperature at 2 cm depth did not exceed 20 °C at the clearing. Comparison of the maximal fluxes measured in the laboratory ($0.025\,\mathrm{nmol\,m^{-2}\,s^{-1}}$) with maximal fluxes calculated from soil nitrite (0.35–0.99 $\mathrm{mg\,kg^{-1}}$ in terms of N) and pH (3.0–3.4) values ($F(\mathrm{HONO_{max}}) = 1810\,\mathrm{nmol\,m^{-2}\,s^{-1}}$) according to Su et al. (2011) reveals that the measured fluxes are at least 4 orders of magnitude lower. For the calculations we used a gravimetric soil water content of $\vartheta_{\mathrm{soil}} = 0.2\,\mathrm{kg\,kg^{-1}}$ and a transfer velocity (v_{tr}) of $1\,\mathrm{cm\,s^{-1}}$ (Su et al., 2011), and measured pH and nitrite values (see Table S1). The discrepancy between our measurements and the calculations according to Su et al. (2011) decreases to about a factor of 50 when v_{tr} is determined for our measurement setup instead of using a fixed value of $1\,\mathrm{cm\,s^{-1}}$. The transfer velocity v_{tr} was determined by calculating the soil resistance according to Moldrup et al. (2000) from measured soil properties for the Waldstein site (Bargsten et al., 2010) and using the aerodynamic resistance ($R_{\mathrm{aero}} = 90\,\mathrm{s\,m^{-1}}$) from a chamber system of similar design and dimensions (Pape et al., 2009). This comparison emphasizes the importance of explicitly considering mass transfer between the soil and atmosphere. Additionally, based on soil nitrite ($\sim 1\,\mu\mathrm{g\,g^{-1}}$ N) and pH (~ 3) values at our site, one would expect rather high HONO emissions according to the acid–base and Henry's law equilibrium. Hence, it seems more likely that microbes are directly involved in the HONO formation as proposed by Oswald et al. (2013), but microbial activity in our samples was low due to the low pH (~ 3) of the organic soil (e.g. Matthies et al., 1997; de Boer and Kowalchuk, 2001; Rousk et al., 2010). Maljanen et al. (2013) found that some acidic forest soils emit measurable amounts of HONO and, thus, proposed nitrogen availability for the microbes as an important factor controlling HONO emissions. The mechanisms controlling HONO emissions from soils (microbial production versus physicochemical release) are still the subject of debate. Maximum emissions for neutral to alkaline soils were attributed to the activity of ammonia-oxidizing bacteria (Oswald et al.2013). Donaldson et al. (2014b) studied the effect of surface acidity of soil particles (in contrast to the bulk soil pH) on HONO uptake. Their study confirmed that the acidity of the particles rather than the bulk pH determined the HONO exchange, which could explain HONO emissions at high (bulk) pH. Nevertheless, this mechanism is applicable to mineral soils only. Another possible effect would be HONO loss in the soil by chemodenitrification as proposed by Clark (1962). During chemodenitrification in the soil, HONO is converted to NO and N_2O depending on pH and organic content, with the highest conversion rates at low pH and high organic content (e.g. Allison, 1963, van Cleemput and Baert, 1984; Ventera et al., 2005). A recent flow tube study (Donaldson et al., 2014a) reports 16 % NO and 13 % N_2O yield from HONO adsorbing to a mineral soil (less than 3 % organic and pH of 6.5). Thus, based on the prior semi-quantitative studies, high loss rates could be expected for the organic soil at our site. Therefore, the acidic conditions of the organic soil at the Waldstein site may lead to additional HONO loss by chemodenitrification and thus low soil HONO emissions.

3.4.2 Light-induced NO_2 conversion

HONO fluxes from light-induced NO_2 conversion were calculated by assuming that the flux from the surface equals the chemical formation at the surface. HONO is formed by reactive collisions of NO_2 with the humic acid surface, and Stemmler et al. (2007) defined their uptake coefficient (γ_{rxn}) as the ratio of these reactive collisions to the number of gas-kinetic collisions of NO_2 molecules with the surface. Hence, we calculated the HONO flux by multiplying the number of gas kinetic collisions given by Eq. (1) with the reactive uptake coefficient given by Eq. (2) (Stemmler et al., 2007):

$$Z_w = \frac{n \times \omega}{4}, \tag{1}$$

$$\gamma_{\mathrm{rxn}} = \frac{4}{\omega} \times \frac{1}{9.3 \times 10^{22} \times [\mathrm{NO_2}] \times [F]^{-1} + 2330}, \tag{2}$$

where Z_w is the number of collisions per time (s) and area ($\mathrm{m^2}$), n is the volume number density per $\mathrm{m^3}$, ω is the mean thermal velocity of NO_2 in $\mathrm{m\,s^{-1}}$, $[NO_2]$ is the NO_2 mixing ratio in ppb measured at 10 cm above the surface, and F is the actinic flux in the 400–750 nm range in photons per $\mathrm{m^3}$ and $\mathrm{s^{-1}}$. For simplicity, we used the irradiance in the 400–

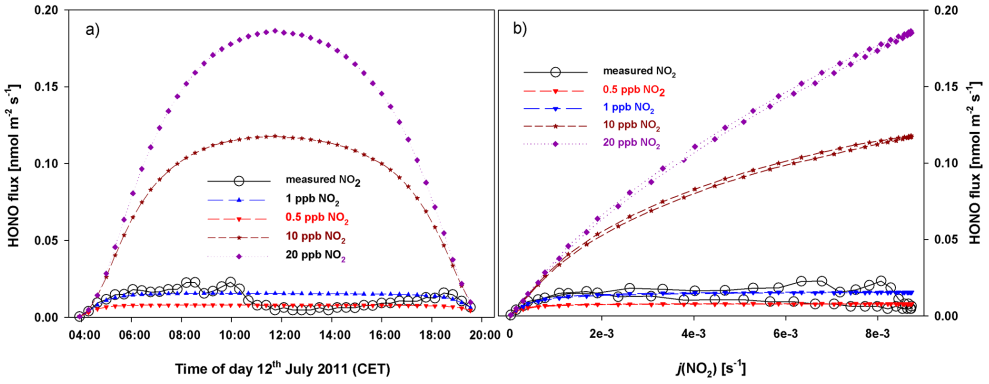

Figure 4. Diurnal cycles of HONO emission fluxes caused by light-induced NO_2 conversion for different NO_2 mixing ratios are shown in panel **(a)**. The corresponding correlations of HONO formation with $j(NO_2)$ are presented in panel **(b)**.

700 nm range (equivalent to the photosynthetic active radiation, PAR) instead of the actinic flux from 400 to 750 nm for F because this value can be directly compared to measurements and to the model output of the TUV model. Furthermore, in the study of Stemmler et al. (2007), the actinic flux of the lamps and absorption of the humic acid was low, in the 700–750 nm wavelength range, thus having little influence on the reactive uptake. Since our simple model assumes a flat surface of 1 m^2 completely covered with humic acid, it is well justified to use the irradiance instead of the actinic flux.

Calculation of the HONO flux using Eqs. (1) and (2) with NO_2 mixing ratios measured 10 cm above the surface and modelled irradiance resulted in light saturation of HONO formation in the early morning at about 07:00 CET and it remains independent of light intensity for most of the day (see Fig. 4). In addition, the saturation itself is dependent on NO_2 with the fastest saturation observed for low NO_2 mixing ratios. Stemmler et al. (2006) explain this behaviour with two competing processes: (a) the light-driven formation of the "reductive centres" that react with NO_2 and (b) the competing light-driven formation of oxidants that deactivate these reductive centres. If more NO_2 is available at the surface the reaction rate increases and the deactivation rate decreases. A saturation of the surface with respect to NO_2 is observed for mixing ratios > 50 ppb (Stemmler et al., 2006, 2007). If this saturation behaviour (with respect to light intensities) also prevails on natural surfaces, at mixing ratios below 1 ppb the unknown HONO source should be solely correlated with NO_2 independent from radiation, which to our knowledge has not been reported up to now. Previous studies found that the unknown HONO source correlated with $j(NO_2)$ or irradiance with only a minor dependence on NO_2 (e.g. Su et al., 2008; Sörgel et al., 2011a; Wong et al., 2012). However, the type and structure of photosensitizers on natural surfaces might differ substantially from a pure humic acid film and, thus, might not be saturated at high light intensities. For example for humic acid dissolved in ice, Bartels-Rausch et al. (2010) did not observe deactivation of the surface uptake. However, only actinic fluxes of up to about 100 W m^{-2} (400–700 nm) were considered, compared to irradiance values of about 400 W m^{-2} in the same wavelength range around noon in our study. Consequently, we consider the light saturation of NO_2 conversion on organic surfaces a key issue for determining the role of this HONO formation pathway in the environment.

3.4.3 Photolysis of adsorbed HNO_3

The photolysis of HNO_3 adsorbed to surfaces has also been suggested as a source of HONO (e.g. Zhou et al., 2002, 2011). We measured the leaf nitrate loadings of young spruce trees (up to 1.6 m height) at the clearing close to the HONO measurement setup. A detailed description of the sampling and the calculations can be found in the Supplement. Unfortunately, measurements of the nitrate loadings on the grass below the HONO inlets are not available, but we assume that they are comparable to the nitrate loadings of the trees. Nitrate loadings at the forest site were not measured, but the contribution of HNO_3 photolysis is expected to be much lower than at the clearing as the available radiation is attenuated by the canopy by a factor of about 10–25 (Sörgel et al., 2011b). Furthermore, we have found no evidence of a HONO source at the forest floor (see Sect. 3.2).

The nitrate loadings of the young spruce trees at the clearing are $1.7 \pm 0.7 \times 10^{-5}$ mol m^{-2}, which is in relatively good agreement with the value of $0.8 \pm 0.3 \times 10^{-5}$ mol m^{-2} reported by Zhou et al. (2011). Both research sites are located in rural forested areas, but considering the influence of different environmental variables, such as NO_x mixing ratios, precipitation intensity and plant surfaces, all of which influence HNO_3 formation and deposition, a variation by a factor of 2 may be expected.

The potential HONO emission fluxes from the photolysis of adsorbed HNO_3 were calculated using three different approaches:

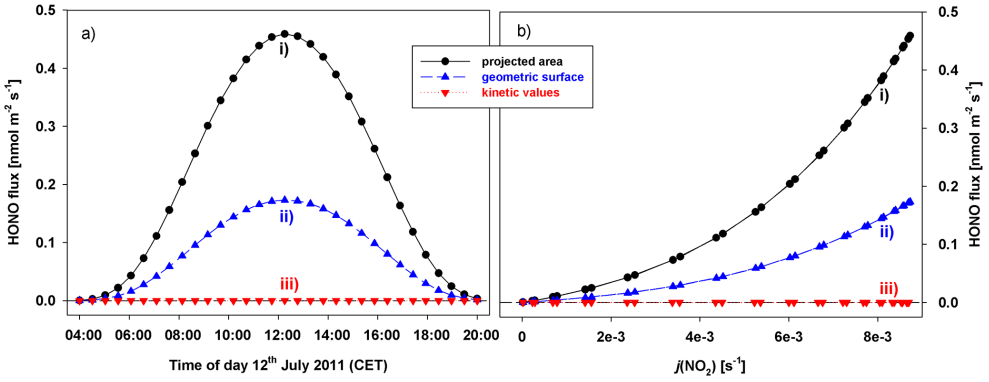

Figure 5. HONO fluxes from photolysis of adsorbed HNO_3 calculated by three different approaches (for details see text). Diurnal cycles of the HONO fluxes are shown in panel **(a)**, whereas panel **(b)** shows the relationship between HONO fluxes and $j(NO_2)$.

1. All measured nitrate represents adsorbed HNO_3 at the top surface of the needles, and HONO formation from photolysis of adsorbed HNO_3 proceeds with an empirical enhancement factor of 43 of $j(HNO_3)$ (Zhou et al., 2011).

2. Similar to approach 1 but the nitrate loading is distributed over the whole geometric surface of the needles (Oren et al., 1986) and, thus, a factor of 2.65 less HNO_3 is exposed to radiation.

3. The photolysis frequency of adsorbed HNO_3 is calculated directly from the absorption cross section of adsorbed HNO_3 on fused silica reported by Zhu et al. (2008) and the corresponding irradiance calculated by the TUV model. This photolysis frequency multiplied with the nitrate loading according to approach 2 yields the NO_2 formed at the surface. Then, HONO formation is calculated as described in Sect. 3.4.2. To derive the reactive uptake coefficient according to Eq. (2) (Stemmler et al., 2007), we used the irradiance integrated over the 290–700 nm wavelength range and calculated the NO_2 concentration which is equivalent to the amount of NO_2 molecules formed at the surface by HNO_3 photolysis.

A comparison of $j(NO_2)$ values from the TUV model with those calculated from global radiation measurements by the approach of Trebs et al. (2009) showed reasonable agreement. The values agree within 8 % around noon.

Figure 5 summarizes the results of the different approaches. Based on empirical factors of light enhancement and HONO formation (Zhou et al., 2011), approaches 1 and 2 yielded a light-dependent HONO source in the same order of magnitude as the estimated HONO fluxes (0.04 ± 0.02 nmol m^{-2} s^{-1}; see Sect. 3). The calculated potential HONO fluxes according to approach 1 are a factor of 2 higher (about 0.46 nmol m^{-2} s^{-1}) than those of Zhou et al. (2011) (0.25 nmol m^{-2} s^{-1}), which is consistent with the twofold-higher nitrate loading measured at our site. However, we consider approach 2 to be more realistic. The diurnal cycle of this source (Fig. 5) follows $j(HNO_3)$ as the mean nitrate loading is used for the calculation. This seems to be valid as we found rather constant surface nitrate loadings during different times of the day (see Fig. S4).

Approach 3, a combination of photolysis of adsorbed HNO_3 and light-induced conversion of the photolysis product NO_2 (see also Sect. 3.4.2) as proposed by Zhou et al. (2011), reveals several interesting findings:

- The calculated photolysis frequency of adsorbed HNO_3 is higher than in the gas phase by a factor of 2000.
- The lifetime of adsorbed HNO_3 with respect to photolysis is only about 15 min at noon.
- NO_2 formed at the surface by HNO_3 photolysis corresponds to a mixing ratio of NO_2 in the gas phase of only a few ppt.

If the strongly enhanced photolysis of adsorbed HNO_3 is valid for natural surfaces, this will have important implications for HNO_3 deposition. HNO_3 would more likely be an intermediate with a lifetime comparable to that of HONO (about 15 min at noon) than a final sink for NO_x. However, even if photolysis of adsorbed HNO_3 is strongly enhanced, formation of HONO would be rather slow if the subsequent reaction of NO_2* (Abida et al., 2012) occurs via the light-induced NO_2 conversion (Stemmler et al., 2006) as proposed by Zhou et al. (2011). As shown in Sect. 3.4.2, the light-induced conversion is light saturated during most of the day especially for low NO_2 mixing ratios. If we compare the number NO_2 molecules formed at the surface through HNO_3 photolysis to the number of NO_2 molecules hitting the surface through gas kinetic collisions this would correspond to a mixing ratio of only a few ppt. Thus, this pathway would not compete with ambient NO_2 for the conditions in our study. Hence, a different NO_2* reaction mechanism must exist to

explain the proposed HONO formation from HNO_3. A potential pathway for NO_2* to form HONO is the reaction with water (e.g. Crowley and Carl, 1997; Amedro et al., 2011). Sörgel et al. (2011a) speculated that the reaction of NO_2* with water at the surface might be faster than the respective gas-phase reaction, which is not of atmospheric importance (e.g. Crowley and Carl, 1997; Sörgel et al., 2011a; Amedro et al., 2011). The formation of NO_2* (either from HNO_3 photolysis or directly in the gas phase) is not the limiting step, as in the gas-phase j values for excitation ($NO_2 \rightarrow NO_2$*) are about a factor of 5 higher under typical tropospheric conditions (Crowley and Carl, 1997) than for photo dissociation of NO_2. The limiting step is the small portion of reactive quenching of NO_2* by water vapour as the majority of excited NO_2 molecules gets deactivated by collision with N_2, O_2 and water vapour. According to Abida et al. (2012), deactivation of NO_2* is much faster at the surface than in the gas phase, thus reducing the probability for reactive quenching with water and formation of HONO. For a quantitative evaluation of this reaction pathway, knowledge of the ratio of deactivation to reactive quenching of surface-adsorbed NO_2* and H_2O is crucial. Another pathway might be the photolysis of nitrate in an aqueous solution that has been reported to yield HONO and NO_2 (Scharko et al., 2014), whereby HONO formation was attributed to efficient hydrolysis of NO_2 that is formed in solution.

3.5 Comparison of calculated fluxes and source estimates

Transferring the HONO formation mechanisms proposed by laboratory measurements to field conditions involves uncertainties as discussed in detail in the previous sections. However, except for HNO_3 photolysis (Zhou et al., 2011) these source mechanisms have not been quantified in field studies up to now. Furthermore, to our knowledge the various reactions have not been studied under natural conditions, except for a proof of principle study with irradiated bare soil as a natural humic acid environment (Stemmler et al., 2006), and the empirically derived HNO_3 conversion factors (Zhou et al., 2003). In Fig. 6 all source estimates and the observed flux estimates from the field are summarized. The main findings are (a) that all sources are within the same order of magnitude, and (b) due to the large systematic uncertainties of the source estimates and the potentially large errors of the flux estimates, none of the sources can be favoured or excluded.

The soil flux was the only source to be measured directly, and these measurements were performed in the laboratory. The soil HONO flux would likely be lower in the field as the soil at the site was covered by vegetation which can take up HONO (Schimang et al., 2006) and because ambient HONO mixing ratios were above zero. NO_2 mixing ratios dropped below 500 ppt in the afternoon, leading to very low HONO fluxes from light-induced NO_2 conversion. Surprisingly, this photochemical source did not show a diurnal

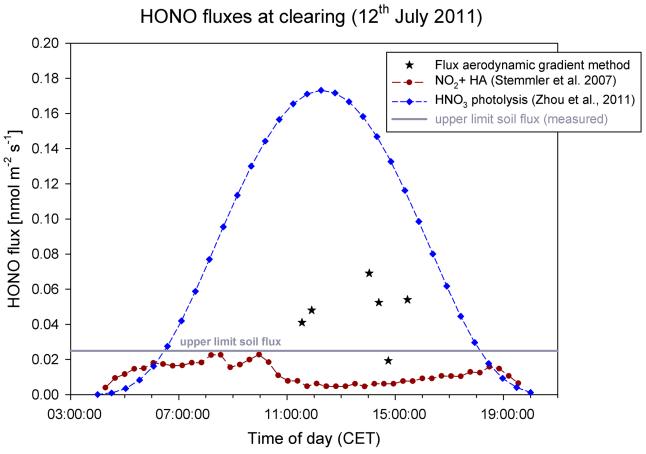

Figure 6. Comparison of measured HONO fluxes at the clearing on 12 July 2012 with estimates of potential HONO sources. Black stars represent the fluxes derived from the aerodynamic gradient method. Blue diamonds are HONO fluxes calculated from the measured nitrate loadings according to Zhou et al. (2011) but using the geometric needle area (see Sect. 3.4.3, approach 2). Brown dots are calculated HONO fluxes according to Stemmler et al. (2007) assuming a flat surface covered with humic acid. The grey horizontal line marks the upper limit of soil HONO fluxes derived from laboratory dynamic chamber measurements.

cycle but became light saturated early in the morning and, thus, was solely dependent on NO_2 mixing ratios. It remains an open question whether light saturation also occurs on natural surfaces. The photolysis of adsorbed HNO_3 produced considerable HONO fluxes (even for approach 2, Sect. 3.4.3) when using an empirically derived HONO conversion factor (Zhou et al., 2003, 2011). In contrast, the proposed mechanism based on reaction kinetics (approach 3, Sect. 3.4.3) failed to produce considerable amounts of HONO. Although some of the sources were unexpectedly small, the combination of all three sources yields much higher fluxes than measured in the field. This may be attributed to enhanced deposition of HONO during the day due to stomata opening and take-up by plants (Schimang et al., 2006), which would reduce measured net emission fluxes. However, the contribution of daytime deposition has not been measured up to now.

4 Conclusions

Our results reveal that the forest floor was predominantly a net sink for HONO, and the clearing constitutes a net sink for HONO during nighttime and a net source during daytime. Hence, net sources and net sinks coexist in heterogeneous landscapes.

HONO emissions calculated for three proposed mechanisms agreed with the measured fluxes within 1 order of magnitude. On the one hand, this shows that the postulated sources are of the right order of magnitude, but on the other

hand, even the presented comprehensive data set including vertical profiles is not sufficient to exclude or confirm one individual source. The detailed investigation of three potential HONO sources, i.e. soil emissions, NO_2 conversion with humic acids and photolysis of adsorbed HNO_3, revealed important findings:

- Soil emissions were found to be several orders of magnitude lower than would be expected from the model of Su et al. (2011), and calculated fluxes are very sensitive to the parameterization of mass transfer from the soil to the atmosphere. Furthermore, acidic soils do not necessarily favour HONO emissions. Emissions are a factor of 700 higher for agricultural soils (Oswald et al., 2013) and thus might be highly influenced by microbial activities.

- NO_2 conversion on humic acid surfaces was found to be light saturated from the early morning throughout most of the daytime under ambient conditions and, thus, only dependent on NO_2. This saturation effect has not been observed in field measurements up to now. Consequently, we could not identify the expected correlation of HONO formation with $j(NO_2)$ for this reaction. Furthermore, at low NO_2 levels this source is very small at our site.

- Photolysis of adsorbed HNO_3 was found to explain the estimated HONO fluxes when using an empirical parameterization for HONO formation, but it failed to produce noticeable amounts of HONO when the formation was calculated according to the proposed mechanism and literature values for adsorption cross sections and reaction kinetics.

Since HNO_3 photolysis is not correlated to $j(NO_2)$ either, the correlation of the unknown HONO source to $j(NO_2)$ as observed for example by Su et al. (2008) and Sörgel et al. (2011a) might originate from the unbalanced photolytic loss term of HONO ($j(HONO) \times [HONO]$). This loss term is highly correlated to $j(NO_2)$ in the budget calculations (Oswald et al., 2015), and is generally interpreted as the unknown source. Recently, an internal source of HONO in the boundary layer from the interconversion between NO_x and HO_x has been postulated to have a contribution of about 75 % (Li et al., 2014). Such a source would explain the observed correlation to $j(NO_2)$ or $j(HONO)$. In our study, the surface emission flux of HONO is only in the order of a few percent of the calculated photolytic loss within the boundary layer, which is even less than estimated from boundary layer profile measurements ($\sim$ 20 % ground contribution; Zhang et al., 2009; Li et al., 2014).

However, a daytime ground source of HONO exists that can produce additional OH, thus enhancing the oxidation capacity of the lower troposphere. The relative contributions of ground sources and volume sources and, hence, the contribution of HONO to primary OH formation remains to be quantified by combining field measurements with the application of chemistry and transport models.

The Supplement related to this article is available online at doi:10.5194/acp-15-9237-2015-supplement.

Acknowledgements. The authors gratefully acknowledge financial support by the German Science Foundation (DFG project HE 5214/4-1) and by the Max Planck Society. We would like to acknowledge the Department of Micrometeorology of the University of Bayreuth for the eddy flux measurements during IOP-3 and the meteorological data from the Pflanzgarten site. Ground cover types and plant area data are courtesy of Eva Falge and Linda Voss. We are grateful to Robert Oswald for checking and assisting with the calculations regarding the soil emissions. Erica Duran helped with the nitrate loading sampling and calculated the needle areas. We thank Tracey Andreae for proofreading the manuscript.

The article processing charges for this open-access publication were covered by the Max Planck Society.

Edited by: R. McLaren

References

Abida, O., Du, J., and Zhu, L.: Investigation of the photolysis of the surface-adsorbed HNO_3 by combining laser photolysis with Brewster angle cavity ring-down spectroscopy, Chem. Phys. Lett., 534, 77–82, 2012.

Alicke, B., Geyer, A., Hofzumahaus, A., Holland, F., Konrad, S., Pätz, H. W., Schäfer, J., Stutz, J., Volz-Thomas, A., and Platt, U.: OH formation by HONO photolysis during the BERLIOZ experiment, J. Geophys. Res., 108, 8247, doi:10.1029/2001JD000579, 2003.

Allison, F.: Losses of gaseous nitrogen from soils by chemical mechanisms involving nitrous acid and nitrites, Soil Sci., 96, 404–409, 1963.

Amedro, D., Parker, A. E., Schoemaecker, C., and Fittschen, C.: Direct observation of OH radicals after 565 nm multi-photon excitation of NO_2 in the presence of H_2O, Chem. Phys. Lett., 513, 12–16, 2011.

Arens, F., Gutzwiller, L., Baltensperger, U. R., Gäggler, H. W., and Ammann, M.: Heterogeneous reaction of NO_2 on diesel soot particles, Environ. Sci. Technol., 35, 2191–2199, 2001.

Aubin, D. G. and Abbatt, J. P. D.: Interaction of NO_2 with hydrocarbon soot: focus on HONO yield, surface modification, and mechanism, J. Phys. Chem. A, 111, 6263–6273, 2007.

Bargsten, A., Falge, E., Pritsch, K., Huwe, B., and Meixner, F. X.: Laboratory measurements of nitric oxide release from forest soil with a thick organic layer under different understory types, Biogeosciences, 7, 1425–1441, doi:10.5194/bg-7-1425-2010, 2010.

Bartels-Rausch, T., Brigante, M., Elshorbany, Y. F., Ammann, M., D'Anna, B., George, C., Stemmler, K., Ndour, M., and Kleff-

mann, J.: Humic acid in ice: Photo-enhanced conversion of nitrogen dioxide into nitrous acid, Atmos. Environ., 44, 5443–5450, 2010.

Bejan, I., Aal, Y. A. E., Barnes, I., Benter, T., Bohn, B., Wiesen, P., and Kleffmann, J.: The photolysis of ortho-nitrophenols: a new gas phase source of HONO, Phys. Chem. Chem. Phys., 8, 2028–2035, doi:10.1039/b516590c, 2006.

Clark, F. E.: Losses of nitrogen accompanying nitrification, Transactions of the International Society of Soil Science, Communications IV and V, Lower Hutt, New Zealand, 173–176, 1962.

Colussi, A. J., Enami, S., Yabushita, A., Hoffmann, M. R., Liu, W.-G., Mishraaf, H., and Goddard, W. A.: Tropospheric aerosol as a reactive intermediate, Faraday Discuss., 165, 407–420, 2013.

Cox, R. A.: The photolysis of nitrous acid in the presence of carbon monoxide and sulphur dioxide, J. Photochem., 3, 291–304, 1974.

Crowley, J. N. and Carl, S. A.: OH formation in the photoexcitation of NO_2 beyond the dissociation threshold in the presence of water vapor, J. Phys. Chem. A, 101, 4178–4184, 1997.

Czader, B. H., Rappenglück, B., Percell, P., Byun, D. W., Ngan, F., and Kim, S.: Modeling nitrous acid and its impact on ozone and hydroxyl radical during the Texas Air Quality Study 2006, Atmos. Chem. Phys., 12, 6939–6951, doi:10.5194/acp-12-6939-2012, 2012.

De Boer, W. and Kowalchuk, G. A.: Nitrification in acid soils: micro-organisms and mechanisms, Soil Biol. Biochem., 33, 853–866, 2001.

De Jesus Medeiros, D. and Pimentel, A. S.: New insights in the atmospheric HONO formation: New pathways for N_2O_4 isomerization and NO_2 dimerization in the presence of water, J. Phys. Chem. A, 115, 6357–6365, 2011.

Donaldson, M. A., Berke, A. E., and Raff, J. D.: Uptake of Gas Phase Nitrous Acid onto Boundary Layer Soil Surfaces, Environ. Sci. Technol., 48, 375–383, doi:10.1021/es404156a, 2014a.

Donaldson, M. A., Bish, D. L., and Raff, J. D.: Soil surface acidity plays a determining role in the atmospheric-terrestrial exchange of nitrous acid, P. Natl. Acad. Sci. USA, 111, 18472–18477, doi:10.1073/pnas.1418545112, 2014b.

Febo, A., Perrino, C., and Allegrini, I.: Measurement of nitrous acid in Milan, Italy, by DOAS and diffusion denuders, Atmos. Environ., 30 3599–3609, 1996.

Finlayson-Pitts, B. J.: Reactions at surfaces in the atmosphere: integration of experiments and theory as necessary (but not necessarily sufficient) for predicting the physical chemistry of aerosols, Phys. Chem. Chem. Phys., 11, 7760–7779, 2009.

Finlayson-Pitts, B. J., Wingen, L. M., Sumner, A. L., Syomin, D., and Ramazan, K. A.: The heterogeneous hydrolysis of NO_2 in laboratory systems and in outdoor and indoor atmospheres: An integrated mechanism, Phys. Chem. Chem. Phys., 5, 223–242, 2003.

Foken, T.: Lufthygienisch-bioklimatische Kennzeichnung des oberen Egertales (Fichtelgebirge bis Karlovy Vary), Bayreuther Forum Ökologie, 100, Bayreuth, Germany, 70 pp., 2003.

Foken, T: Micrometeorology, Springer, Heidelberg, Germany, 308 pp., 2008.

Foken, T., Meixner, F. X., Falge, E., Zetzsch, C., Serafimovich, A., Bargsten, A., Behrendt, T., Biermann, T., Breuninger, C., Dix, S., Gerken, T., Hunner, M., Lehmann-Pape, L., Hens, K., Jocher, G., Kesselmeier, J., Lüers, J., Mayer, J.-C., Moravek, A., Plake, D., Riederer, M., Rütz, F., Scheibe, M., Siebicke, L., Sörgel, M., Staudt, K., Trebs, I., Tsokankunku, A., Welling, M., Wolff, V., and Zhu, Z.: Coupling processes and exchange of energy and reactive and non-reactive trace gases at a forest site – results of the EGER experiment, Atmos. Chem. Phys., 12, 1923–1950, doi:10.5194/acp-12-1923-2012, 2012.

George, C., Strekowski, R. S., Kleffmann, J., Stemmler, K., and Ammann, M.: Photoenhanced uptake of gaseous NO_2 on solid organic compounds: a photochemical source of HONO?, Faraday Discuss., 130, 195–210, 2005.

Gustafsson, R. J., Kyriakou, G., and Lambert, R. M.: The molecular mechanism of tropospheric nitrous acid production on mineral dust surfaces, ChemPhysChem, 9, 1390–1393, 2008.

Gutzwiller, L., George, C., Rössler, E., and Ammann, M.: Reaction kinetics of NO_2 with resorcinol and 2,7-naphthalenediol in the aqueous phase at different pH, J. Phys. Chem. A, 106, 12045–12050, 2002.

Harrison, R. M. and Kitto, A.-M. N.: Evidence for a surface source of atmospheric nitrous acid, Atmos. Environ., 28, 1089–1094, 1994.

Harrison, R. M., Peak, J. D., and Collin, G. M.: Tropospheric cycle of nitrous acid, J. Geophys. Res., 101, 14429–14439, 1996.

Heland, J., Kleffmann, J., Kurtenbach, R., and Wiesen, P.: A new instrument to measure gaseous nitrous acid (HONO) in the atmosphere, Environ. Sci. Technol., 35, 3207–3212, 2001.

Kamboures, M. A., Raff, J. D., Miller, Y., Phillips, L. F., Finlayson-Pitts, B. J., and Gerber, R. B.: Complexes of HNO_3 and NO_3 with NO_2 and N_2O_4, and their potential role in atmospheric HONO formation, Phys. Chem. Chem. Phys., 10, 6019–6032, 2008.

Kleffmann, J.: Daytime sources of nitrous acid (HONO) in the atmospheric boundary layer, ChemPhysChem, 8, 1137–1144, 2007.

Kleffmann, J., Becker, K. H., Lackhoff, M., and Wiesen, P.: Heterogeneous conversion of NO_2 on carbonaceous surfaces, Phys. Chem. Chem. Phys., 1, 5443–5450, 1999.

Kleffmann, J., Heland, J., Kurtenbach, R., Lörzer, J., and Wiesen, P.: A new instrument (LOPAP) for the detection of nitrous acid (HONO), Environ. Sci. Pollut. R., 4, 48–54, 2002.

Kleffmann, J., Gavriloaiei, T., Hofzumahaus, A., Holland, F., Koppmann, R., Rupp, L., Schlosser, E., Siese, M., and Wahner, A.: Daytime formation of nitrous acid: A major source of OH radicals in a forest, Geophys. Res. Lett., 32, L05818, doi:10.1029/2005GL022524, 2005.

Kubota, M. and Asami, T.: Source of nitrous acid volatilized from upland soils, Soil Sci. Plant Nutr., 31, 35–42, 1985.

Lee, B. H., Wood, E. C., Herndon, S. C., Lefer, B. L., Luke, W. T., Brune, W. H., Nelson, D. D., Zahniser, M. S., and Munger, J. W.: Urban measurements of atmospheric nitrous acid: A caveat on the interpretation of the HONO photostationary state, J. Geophys. Res., 118, 1–8, doi:10.1002/2013JD020341, 2013.

Li, X., Rohrer, F., Hofzumahaus, H., Brauers, T., Häseler, R., Bohn, B., Broch, S., Fuchs, H., Gomm, S., Holland, F., Jäger, J., Kaiser, J., Keutsch, F. N., Lohse, I., Lu, K., Tillmann, R., Wegener, R., Wolfe, G. M., F. Mentel, T. F., Kiendler-Scharr, A., and Wahner, A.: Missing gas-phase source of HONO inferred from zeppelin measurements in the troposphere, Science, 344, 292–296, doi:10.1126/science.1248999, 2014.

Ludwig, J., Meixner, F. X., Vogel, B., and Förstner J.: Soil-air exchange of nitric oxide: An overview of processes, environmen-

tal factors, and modeling studies, Biogeochemistry, 52, 225–257, 2001.

Madronich, S. and Flocke, S.: The role of solar radiation in atmospheric chemistry, in The Handbook of Environmental Chemistry/Reactions and Processes/Environmental Photochemistry Part I: BD 2 / Part L, edited by: Boule, P., Springer-Verlag, Heidelberg, Germany, 373, 1–26, 1998.

Maljanen, M., Yli-Pirilä, P., Hytönen, J., Joutsensaari, J., and Martikainen, P. J.: Acidic northern soils as sources of atmospheric nitrous acid (HONO), Soil Biol. Biochem., 67, 94–97, doi:10.1016/j.soilbio.2013.08.013, 2013.

Matthies, C., Erhard, H.-P., and Drake, H. L.: Effects of pH on the comparative culturability of fungi and bacteria from acidic and less acidic forest soils, J. Basic. Microb., 37, 335–343, 1997.

Mauder, M. and Foken, T.: Documentation and instruction manual of the eddy-covariance software package TK3, Universität Bayreuth, Abteilung Mikrometeorologie, 46, 60 pp., ISSN1614-8924, 2011.

Miller, Y., Finlayson-Pitts, B. J., and Gerber, R. B.: Ionization of N_2O_4 in contact with water: mechanism, time scales and atmospheric implications, J. Am. Chem. Soc., 131, 12180–12185, doi:10.1021/ja900350g, 2009.

Moldrup, P., Olesen, T., Gamst, J., Schjonning, P., Yamaguchi, T., and Rolston, D. E.: Predicting the gas diffusion coefficient in repacked soil: Water-induced linear reduction model, Soil Sci. Soc. Am. J., 64, 1588–1594, 2000.

Oren, R., Schulze, E.-D., Matyssek, R., and Zimmermann, R.: Estimating photosynthetic rate and annual carbon gain in conifers from specific leaf weight and leaf biomass, Oecologia, 70, 187–193, 1986.

Oswald, R., Behrendt, T., Ermel, M., Wu, D., Su, H., Cheng, Y., Breuninger, C., Moravek, A., Mougin, Delon, C., Loubet, B., Pommerening-Röser, A., Sörgel, M., Pöschl, U., Hoffmann, T., Andreae, M. O., Meixner, F. X., and Trebs, I.: HONO emissions from soil bacteria as a major source of atmospheric reactive Nitrogen, Science, 341, 1233–1235, doi:10.1126/science.1242266, 2013.

Oswald, R., Ermel, M., Hens, K., Novelli, A., Ouwersloot, H. G., Paasonen, P., Petäjä, T., Sipilä, M., Keronen, P., Bäck, J., Königstedt, R., Hosaynali Beygi, Z., Fischer, H., Bohn, B., Kubistin, D., Harder, H., Martinez, M., Williams, J., Hoffmann, T., Trebs, I., and Sörgel, M.: A comparison of HONO budgets for two measurement heights at a field station within the boreal forest in Finland, Atmos. Chem. Phys., 15, 799–813, doi:10.5194/acp-15-799-2015, 2015.

Pape, L., Ammann, C., Nyfeler-Brunner, A., Spirig, C., Hens, K., and Meixner, F. X.: An automated dynamic chamber system for surface exchange measurement of non-reactive and reactive trace gases of grassland ecosystems, Biogeosciences, 6, 405–429, doi:10.5194/bg-6-405-2009, 2009.

Ramazan, K. A., Syomin, D., and Finlayson-Pitts, B. J.: The photochemical production of HONO during the heterogeneous hydrolysis of NO_2, Phys. Chem. Chem. Phys., 6, 3836–3843, 2004.

Ren, X., Sanders, J. E., Rajendran, A., Weber, R. J., Goldstein, A. H., Pusede, S. E., Browne, E. C., Min, K.-E., and Cohen, R. C.: A relaxed eddy accumulation system for measuring vertical fluxes of nitrous acid, Atmos. Meas. Tech., 4, 2093–2103, doi:10.5194/amt-4-2093-2011, 2011.

Rousk, J., Bååth, E., Brookes, P. C., Lauber, C. L., Lozupone, C., Caporaso, J. G., Knight, R., and Fierer, N.: Soil bacterial and fungal communities across a pH gradient in an arable soil, ISME J., 4, 1340–1351, 2010.

Rubasinghege, G. and Grassian V. H.: Photochemistry of adsorbed nitrate on aluminum oxide particle surfaces, J. Phys. Chem. A, 113, 7818–7825, 2009.

Scharko, N. K., Berke, A. E., and Raff, J. D.: Release of nitrous acid and nitrogen dioxide from nitrate photolysis in acidic aqueous solutions, Environ. Sci. Technol., 48, 11991–12001, doi:10.1021/es503088x, 2014.

Schimang R., Folkers A., Kleffmann J., Kleist E., Miebach M., and Wildt J.: Uptake of Gaseous Nitrous Acid (HONO) by Several Plant Species, Atmos. Environ., 40, 1324–1335, 2006.

Schuttlefield, J., Rubasinghege, G., El-Maazawi, M., Bone, J., and Grassian, V. H.: Photochemistry of adsorbed nitrate, J. Am. Chem. Soc., 130, 12210–12211, 2008.

Sörgel, M., Regelin, E., Bozem, H., Diesch, J.-M., Drewnick, F., Fischer, H., Harder, H., Held, A., Hosaynali-Beygi, Z., Martinez, M., and Zetzsch, C.: Quantification of the unknown HONO daytime source and its relation to NO_2, Atmos. Chem. Phys., 11, 10433–10447, doi:10.5194/acp-11-10433-2011, 2011a.

Sörgel, M., Trebs, I., Serafimovich, A., Moravek, A., Held, A., and Zetzsch, C.: Simultaneous HONO measurements in and above a forest canopy: influence of turbulent exchange on mixing ratio differences, Atmos. Chem. Phys., 11, 841–855, doi:10.5194/acp-11-841-2011, 2011b.

Stemmler, K., Ammann, M., Donders, C., Kleffmann, J., and George, C.: Photosensitized reduction of nitrogen dioxide on humic acid as a source of nitrous acid, Nature, 440, 195–198, 2006.

Stemmler, K., Ndour, M., Elshorbany, Y., Kleffmann, J., D'Anna, B., George, C., Bohn, B., and Ammann, M.: Light induced conversion of nitrogen dioxide into nitrous acid on submicron humic acid aerosol, Atmos. Chem. Phys., 7, 4237–4248, doi:10.5194/acp-7-4237-2007, 2007.

Stutz, J., Alicke, B., and Neftel, A.: Nitrous acid formation in the urban atmosphere: Gradient measurements of NO_2 and HONO over grass in Milan, Italy, J. Geophys. Res., 107, 8192, doi:10.1029/2001JD000390, 2002.

Su, H., Cheng, Y. F., Shao, M., Gao, D. F., Yu, Z. Y., Zeng, L. M., Slanina, J., Zhang, Y. H., and Wiedensohler, A.: Nitrous acid (HONO) and its daytime sources at a rural site during the 2004 PRIDE-PRD experiment in China, J. Geophys. Res., 113, D14312, doi:10.1029/2007JD009060, 2008.

Su, H., Cheng,Y., Oswald, R., Behrendt, T., Trebs, I., Meixner, F.-X., Andreae, M. O., Cheng, P., Zhang, Y., and Pöschl, U.: Soil nitrite as a source of atmospheric HONO and OH radicals, Science, 333, 1616–1618, doi:10.1126/science.1207687, 2011.

Trebs, I., Bohn, B., Ammann, C., Rummel, U., Blumthaler, M., Königstedt, R., Meixner, F. X., Fan, S., and Andreae, M. O.: Relationship between the NO_2 photolysis frequency and the solar global irradiance, Atmos. Meas. Tech., 2, 725–739, doi:10.5194/amt-2-725-2009, 2009.

Van Cleemput, O. and Baert, L.: Nitrite: a key compound in N loss processes under acid conditions?, Plant Soil, 76, 233–241, 1984.

VandenBoer, T. C., Brown, S. S., Murphy, J. G., Keene, W. C., Young, C. J., Pszenny, A. A. P., Kim, S., Warneke, C., de Gouw, J. A., Maben, J. R., Wagner, N. L., Riedel, T. P., Thornton, J. A., Wolfe, D. E., Dubé, W. P., Öztürk, F., Brock, C. A.,

Grossberg, N., Lefer, B., Lerner, B., Middlebrook, A. M., and Roberts, J. M.: Understanding the role of the ground surface in HONO vertical structure: High resolution vertical profiles during NACHTT-11, J. Geophys. Res.-Atmos., 118, 10155–10171, doi:10.1002/jgrd.50721, 2013.

VandenBoer, T. C., Young, C. J., Talukdar, R. K., Markovic, M. Z., Brown, S. S., Roberts, J. M., and Murphy, J. G.: Nocturnal loss and daytime source of nitrous acid through reactive uptake and displacement, Nat. Geosci., 8, 5–7, doi:10.1038/ngeo2315, 2015.

Venterea, R. T., Rolston, D. E., and Cardon, Z. G.: Effects of soil moisture, physical, and chemical characteristics on abiotic nitric oxide production, Nutr. Cycl. Agroecosys., 72, 27–40, 2005.

Volkamer, R., Sheehy, P., Molina, L. T., and Molina, M. J.: Oxidative capacity of the Mexico City atmosphere – Part 1: A radical source perspective, Atmos. Chem. Phys., 10, 6969–6991, doi:10.5194/acp-10-6969-2010, 2010.

Wolff, V., Trebs, I., Ammann, C., and Meixner, F. X.: Aerodynamic gradient measurements of the NH_3-HNO_3-NH_4NO_3 triad using a wet chemical instrument: an analysis of precision requirements and flux errors, Atmos. Meas. Tech., 3, 187–208, doi:10.5194/amt-3-187-2010, 2010.

Wong, K. W., Oh, H.-J., Lefer, B. L., Rappenglück, B., and Stutz, J.: Vertical profiles of nitrous acid in the nocturnal urban atmosphere of Houston, TX, Atmos. Chem. Phys., 11, 3595–3609, doi:10.5194/acp-11-3595-2011, 2011.

Wong, K. W., Tsai, C., Lefer, B., Haman, C., Grossberg, N., Brune, W. H., Ren, X., Luke, W., and Stutz, J.: Daytime HONO vertical gradients during SHARP 2009 in Houston, TX, Atmos. Chem. Phys., 12, 635–652, doi:10.5194/acp-12-635-2012, 2012.

Wong, K. W., Tsai, C., Lefer, B., Grossberg, N., and Stutz, J.: Modeling of daytime HONO vertical gradients during SHARP 2009, Atmos. Chem. Phys., 13, 3587–3601, doi:10.5194/acp-13-3587-2013, 2013.

Yabushita, A., Enami, S., Sakamoto, Y., Kawasaki, M., Hoffmann, M. R., and Colussi, A. J.: Anion-catalyzed dissolution of NO_2 on aqueous microdroplets, J. Phys. Chem. A, 113, 4844–4848, 2009.

Zhang, N., Zhou, X., Shepson, P. B., Gao, H., Alaghmand, M., and Stirm, B.: Aircraft measurement of HONO vertical profiles over a forested region, Geophys. Res. Lett., 36, L15820, doi:10.1029/2009GL038999, 2009.

Zhang, N., Zhou, X., Bertman, S., Tang, D., Alaghmand, M., Shepson, P. B., and Carroll, M. A.: Measurements of ambient HONO concentrations and vertical HONO flux above a northern Michigan forest canopy, Atmos. Chem. Phys., 12, 8285–8296, doi:10.5194/acp-12-8285-2012, 2012.

Zhou, X., He, Y., Huang, G., Thornberry, T. D., Carroll, M. A., and Bertman, S. B.: Photochemical production of nitrous acid on glass sample manifold surface, Geophys. Res. Lett., 29, 1681, doi:10.1029/2002GL015080, 2002.

Zhou, X., Gao, H., He, Y., Huang, G., Bertman, S. B., Civerolo, K., and Schwab, J.: Nitric acid photolysis on surfaces in low-NOx environments: Significant atmospheric implications, Geophys. Res. Lett., 30, 1–4, 2003.

Zhou, X. L., Zhang, N., TerAvest, M., Tang, D., Hou, J., Bertman, S., Alaghmand, M., Shepson, P. B., Carroll, M. A., Griffith, S., Dusanter, S., and Stevens, P. S.: Nitric acid photolysis on forest canopy surface as a source for tropospheric nitrous acid, Nat. Geosci., 4, 440–443, doi:10.1038/ngeo1164, 2011.

Zhu, C., Xiang, B., Zhu, L., and Cole, R.: Determination of absorption cross sections of surface-adsorbed HNO_3 in the 290–330 nm region by Brewster angle cavity ring-down spectroscopy, Chem. Phys. Lett., 458, 73–377, 2008.

Zhu, C., Xiang, B., Chu, L. T., and Zhu, L.: Photolysis of Nitric Acid in the Gas Phase, on Aluminum Surfaces, and on Ice Films, J. Phys. Chem. A, 114, 2561–2568, 2010.